

## Relationship between the biodistributions of radioactive metal nuclides in tumor tissue and the physicochemical properties of these metal ions

Atsushi ANDO,\* Itsuko ANDO,\* Shigeru SANADA,\* Tatsunosuke HIRAKI,\*  
Tetsuo TAKEUCHI,\*\* Kinichi HISADA\*\* and Norihisa TONAMI\*\*

\*School of Health Sciences and \*\*School of Medicine, Faculty of Medicine, Kanazawa University

This study was undertaken to elucidate the relationship between the biodistribution of radioactive metal nuclides in tumor tissue and its physicochemical properties.

Potassium analogs ( $^{86}\text{Rb}$ ,  $^{134}\text{Cs}$ ,  $^{201}\text{Tl}$ ) were taken up into viable tumor tissue, although  $^{22}\text{Na}$  concentrated in necrotic tumor tissue.  $^{67}\text{Ga}$  and  $^{111}\text{In}$  were more predominant in inflammatory tissue than in the viable and necrotic tumor tissue.  $^{169}\text{Yb}$  and  $^{167}\text{Tm}$  accumulated in viable tumor tissue and tissue containing viable and necrotic tumor tissue.  $^{67}\text{Ga}$ ,  $^{111}\text{In}$ ,  $^{169}\text{Yb}$  and  $^{167}\text{Tm}$  were bound to the acid mucopolysaccharide with a mol. wt. of about 10,000 daltons in the tumor tissue.  $^{46}\text{Sc}$ ,  $^{51}\text{Cr}$ ,  $^{95}\text{Zr}$ ,  $^{181}\text{Hf}$ ,  $^{95}\text{Nb}$ ,  $^{182}\text{Ta}$ , and  $^{103}\text{Ru}$  were highly concentrated in inflammatory tissue and were bound to the acid mucopolysaccharides with a mol. wt. exceeding 40,000 daltons.  $^{65}\text{Zn}$  and  $^{103}\text{Pd}$  concentrated in viable tumor tissue and were bound to the protein in the tissue.

The results suggest that the difference in intra-tumor distribution of these elements is caused by a difference in the binding substances (or status) of these elements in the tissues, and the binding substance is determined by physicochemical properties of the elements. We therefore conclude that the biodistribution of radioactive metal ions in tumor tissue is determined by its own physicochemical properties.

**Key words:** biodistribution, macroautoradiogram, radioactive metal nuclides, physicochemical properties, tumor tissue

### INTRODUCTION

SOME RADIOISOTOPES injected intravenously produce a higher concentration in tumor tissue than in normal tissues.  $^{67}\text{Ga}$ -citrate and  $^{201}\text{Tl}$ -chloride have been used for detection and location by scintiscanning.

Since the discovery of tumor accumulation of radioactive bismuth by Kahn<sup>1</sup> in 1930, a number of radioactive inorganic compounds have been carefully studied by many investigators. These reports have been summarized by Paterson et al.,<sup>2</sup> by Larson,<sup>3</sup> by Lopez-Majano and Alvarez-Cervera.<sup>4</sup>

In 1968 we began to quantitatively determine the

biodistribution of radioactive inorganic compounds in tumor bearing animals. We summarized the biodistribution of 54 elements and 66 compounds in tumor bearing animals as already reported.<sup>5,6</sup> On the other hand, we have been investigating the biodistribution of radioactive metal nuclides in tumor tissue by macroautoradiography.<sup>7,8,13–17</sup>

In this study, metal organic compounds such as  $^{67}\text{Ga}$ -citrate and  $^{95}\text{Zr}$ -oxalate, were classified as inorganic compounds because these metal nuclides were dissociated from these metal organic compounds in the body after intravenous (IV) or intraperitoneal (IP) administration. To date we have investigated the biodistributions of 17 elements in tumor tissue and examined the relationship between the accumulation in tumor tissue and the properties of these metal compounds. We summarized relationship among the biodistribution, the binding substance (or status) of these nuclides in tumor tissue, and the physicochemical properties of these metal ions.

Received June 17, 1998, revision accepted December 24, 1998.

For reprint contact: Atsushi Ando, Ph.D., School of Health Sciences, Faculty of Medicine, Kanazawa University, 5–11–80, Kodatsuno, Kanazawa 920–0942, JAPAN.

## MATERIALS AND METHODS

### *Animals and experimental tumors*

Male Donryu rats weighing 150–200 g underwent subcutaneous implantation of Yoshida sarcoma ( $1 \times 10^8$  cells/0.25 ml) in the right thigh. Five to six days later these animals were used in these experiments.<sup>7,17</sup> Male ddY mice weighing 25–30 g were implanted with Ehrlich tumor ( $5 \times 10^7$  cells/0.1 ml) in the right thigh and used in these experiments 8–10 days later.<sup>7,8,13–17</sup>

### *Radioactive compounds*

<sup>67</sup>Ga-citrate solution (1 ml containing about 7.4 MBq of carrier free <sup>67</sup>Ga) was prepared by diluting <sup>67</sup>Ga-citrate solution (Philips-Duphar Cyclotron and Isotopes Laboratory, Holland) with 0.08 M sodium citrate solution.<sup>7</sup>

<sup>111</sup>In-citrate solution (1 ml containing about 7.4 MBq of carrier free <sup>111</sup>In) was prepared from <sup>111</sup>In-chloride (Nihon Medipysics Co. Ltd., Japan) and 0.08 M sodium citrate solution.<sup>7</sup>

<sup>169</sup>Yb-citrate solution (1 ml containing about 2 MBq and 0.1 μg of Yb) was prepared from <sup>169</sup>Yb-chloride solution (The Radiochemical Centre, England) and 0.08 M sodium citrate solution.<sup>7</sup>

<sup>167</sup>Tm-citrate solution (1 ml containing about 0.37–3.7 MBq of carrier free <sup>167</sup>Tm) was prepared from <sup>167</sup>Tm-chloride solution<sup>8</sup> and 0.08 M sodium citrate solution.<sup>8</sup>

<sup>201</sup>Tl(I)-chloride solution (1 ml containing about 7.4 MBq of carrier free <sup>201</sup>Tl) was prepared from <sup>201</sup>Tl-chloride (Daiichi Radioisotope Labs., Ltd., Japan) and 0.9% NaCl solution.<sup>7</sup>

<sup>22</sup>Na-chloride solution (1 ml containing about 1.1 MBq of carrier free <sup>22</sup>Na) was prepared by neutralizing <sup>22</sup>Na-chloride in 5 M HCl solution (New England Nuclear, Corp., U.S.A.) with 0.1 M NaOH solution and diluted with 0.9% NaCl solution.<sup>7</sup>

<sup>86</sup>Rb-chloride (1 ml containing about 2.6 MBq and 40 μg of Rb) was prepared by neutralizing <sup>86</sup>Rb-chloride in 0.5 M HCl solution (New England Nuclear, Corp., U.S.A.) with 0.1 M NaOH solution and diluted with 0.9% NaCl solution.<sup>7</sup>

<sup>134</sup>Cs-chloride (1 ml containing about 1.1 MBq and 0.3 μg of Cs) was prepared by neutralizing <sup>134</sup>Cs-chloride in 0.5 M HCl solution (New England Nuclear, Corp., U.S.A.) with 0.1 M NaOH solution and diluted with 0.9% NaCl solution.<sup>7</sup>

<sup>46</sup>Sc-citrate solution (1 ml containing about 2 MBq and 1.5 μg of Sc) was prepared by the following procedure: 0.08 M sodium citrate solution (10 ml) was added to 2.0 ml of <sup>46</sup>Sc-chloride in 2 M HCl solution (New England Nuclear, Corp., U.S.A.) and adjusted to pH 8.0 with sodium bicarbonate. After that, it was heated at about 100°C for 10 min.<sup>13</sup>

<sup>51</sup>Cr(III)-chloride solution (1 ml containing about 2.8 MBq and 1 μg of Cr) was prepared by diluting <sup>51</sup>Cr(III)-chloride in 0.1 M HCl solution (Commissariat a L'Energie

Atomique, France) with 0.9% NaCl solution and adjusting to pH 2.0 with 0.1 M HCl.<sup>13</sup>

<sup>95</sup>Zr-oxalate solution (1 ml containing about 0.26–1.5 MBq of carrier free <sup>95</sup>Zr) was prepared from <sup>95</sup>Zr-oxalate in 0.7 M oxalic acid solution (Oak Ridge National Laboratory, U.S.A.) and 0.9% NaCl solution.<sup>15</sup>

<sup>181</sup>Hf-chloride in 0.05 M HCl solution (1 ml containing about 0.74 MBq and 4 μg of Hf) was prepared from <sup>181</sup>Hf in 2 M HCl solution (The Radiochemical Centre, England) and 0.9% NaCl solution.<sup>15</sup>

<sup>103</sup>Ru-chloride in 0.05 M HCl solution (1 ml containing 0.2–0.74 MBq and 50–200 μg of Ru) was prepared from <sup>103</sup>Ru-chloride in 4 M HCl solution (The Radiochemical Centre, England) and 0.9% NaCl solution.<sup>14</sup>

<sup>95</sup>Nb-oxalate solution (1 ml containing about 0.45 MBq of carrier free <sup>95</sup>Nb) was prepared by diluting <sup>95</sup>Nb-oxalate in 0.5% oxalic acid solution (The Radiochemical Centre, England) with 0.15 M sodium oxalate solution.<sup>16</sup>

<sup>182</sup>Ta-oxalate solution (1 ml containing about 0.4 MBq and about 2.3 μg of Ta) was prepared by diluting <sup>182</sup>Ta-oxalate in 1.2% oxalic acid solution (The Radiochemical Centre, England) with 0.15 M sodium oxalate solution.<sup>16</sup>

<sup>65</sup>Zn-chloride solution (1 ml containing about 0.4 MBq of carrier free <sup>65</sup>Zn) was prepared from <sup>65</sup>Zn-chloride in 0.5 M HCl solution (New England Nuclear, Corp., U.S.A.) and 0.9% NaCl solution.<sup>17</sup>

<sup>103</sup>Pd-chloride solution (1 ml containing about 0.4 MBq of carrier free <sup>103</sup>Pd) was prepared from <sup>103</sup>Pd-chloride in 1 M HCl solution (The Radiochemical Centre, England) and 0.9% NaCl solution.<sup>17</sup>

### *Methods*<sup>7,8,13–17</sup>

Each preparation was injected intravenously through the tail vein of rats and injected intraperitoneally into the mice. These animals were killed and tumor tissue was excised at three, twenty-four and forty-eight hours after the injection of the radioactive compounds. These tissues were embedded in two percent carboxymethyl cellulose sodium salts and frozen with dry ice-acetone (–70°C) immediately after excision. Following this, the frozen tissues were cut into thin serial sections (10 μm) in a cryostat (–20°C). One of these sections was then placed on X-ray film which was developed after an exposure of several days, a second section was fixed in ethanol, and then stained with hematoxylin-eosin.

## RESULTS

### *Biodistribution in tumor tissue*

Hematoxylin-eosin stained sections were divided into the following four categories: 1) viable tumor tissue, 2) tissue containing viable and necrotic tumor tissue, 3) necrotic tumor tissue, 4) connective tissue which contained inflammatory tissue. The relationship between morphological specimens of tumor tissue and accumulation of nuclides was determined from the autoradiogram and

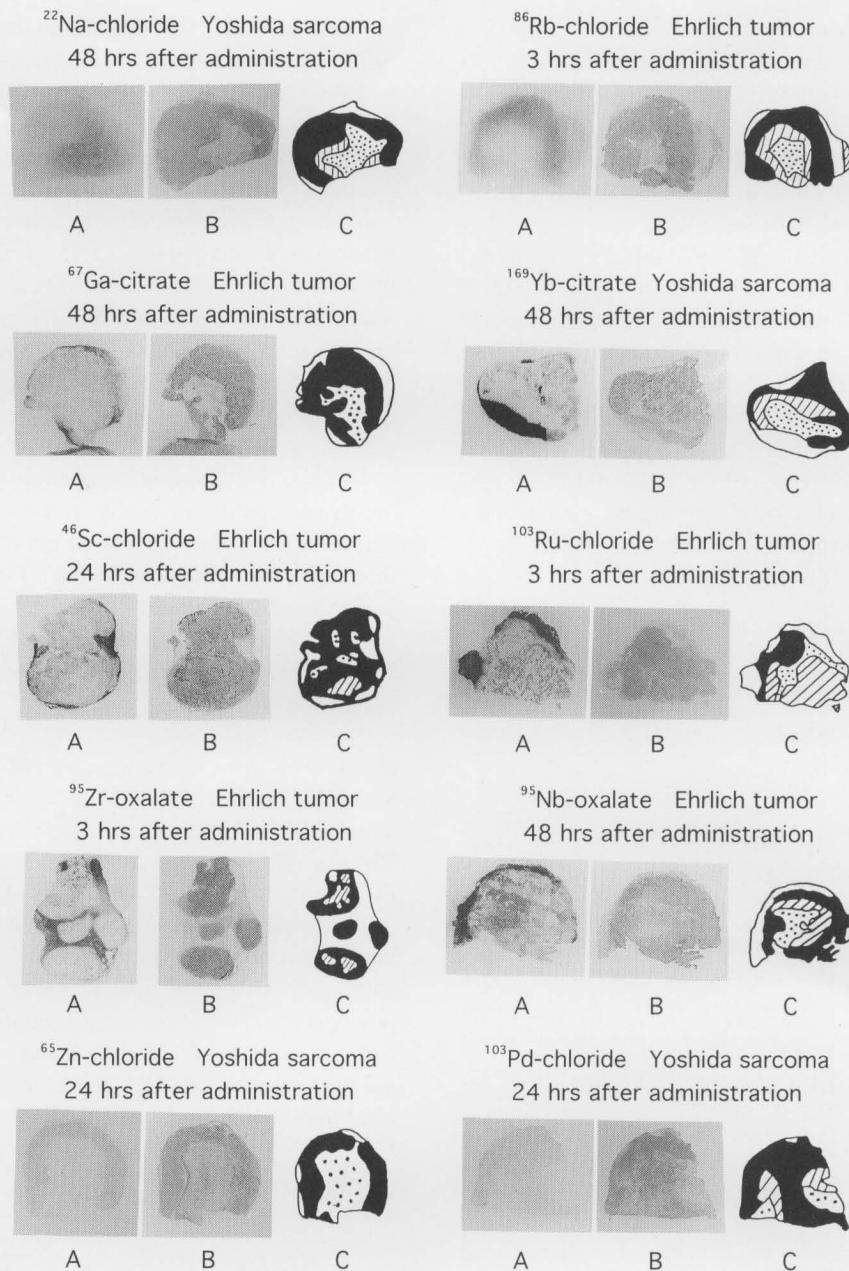


Fig. 1 Morphological specimens.<sup>7,13-17</sup>

A: Macroautoradiogram, B: Hematoxylin-Eosin staining, C: Sketch illustration

■ Viable tumor tissue, ▨ Tissue containing viable and necrotic tumor tissue, ▤ Necrotic tumor tissue, □ Connective tissue (containing inflammatory tissue)

hematoxylin-eosin stained sections.

$^{22}\text{Na}$ : Figure 1 shows a typical autoradiogram, hematoxylin-eosin staining tissue and its sketch illustration of Yoshida sarcoma treated with  $^{22}\text{NaCl}$ . The accumulation of  $^{22}\text{Na}$  was seen in the necrotic tumor tissue and was not seen in the viable tumor tissue or connective tissue.<sup>7</sup>

$^{86}\text{Rb}$ ,  $^{134}\text{Cs}$  and  $^{201}\text{Tl}$ : Figure 1 shows the result for  $^{86}\text{Rb}$ . A large amount of  $^{86}\text{Rb}$  accumulated in the viable tumor tissue and was not seen in the necrotic tumor tissue. A small amount of this nuclide accumulated in the connective tissue and tissue containing viable and necrotic

tumor tissue. Biodistributions of  $^{134}\text{Cs}$  and  $^{201}\text{Tl}$  were very similar to that of  $^{86}\text{Rb}$ .<sup>7</sup>

$^{67}\text{Ga}$  and  $^{111}\text{In}$ : Figure 1 shows the result for  $^{67}\text{Ga}$ . The accumulation of  $^{67}\text{Ga}$  was predominant in connective tissue (especially inflammatory tissue) rather than in the viable tumor tissue, and was hardly seen in necrotic tumor tissue. Distribution of  $^{111}\text{In}$  was very similar to that of  $^{67}\text{Ga}$ .<sup>7</sup>

$^{169}\text{Yb}$  and  $^{167}\text{Tm}$ : Figure 1 shows the result for  $^{169}\text{Yb}$ . A large amount of this nuclide accumulated in viable tumor tissue and the tissue containing viable and necrotic tumor

tissue. Fairly large amounts of this nuclide accumulated in the connective tissue which contained inflammatory tissue. But  $^{169}\text{Yb}$  was not seen in the necrotic tumor tissue regardless of the species of malignant tumor.<sup>7</sup> In the case of  $^{167}\text{Tm}$ , very similar results were obtained.<sup>8</sup> Biodistributions of  $^{169}\text{Yb}$  and  $^{167}\text{Tm}$  in tumor tissue differed only slightly from those of  $^{67}\text{Ga}$  and  $^{111}\text{In}$ .

$^{46}\text{Sc}$ ,  $^{51}\text{Cr}$ ,  $^{103}\text{Ru}$ ,  $^{95}\text{Zr}$ ,  $^{181}\text{Hf}$ ,  $^{95}\text{Nb}$  and  $^{182}\text{Ta}$ : Figure 1 shows the result for  $^{46}\text{Sc}$ .  $^{46}\text{Sc}$  accumulated much more avidly in connective tissue (especially inflammatory tissue) than in viable tumor tissue and necrotic tumor tissue, regardless of the species of malignant tumor.<sup>13</sup> Figure 1 shows the results for  $^{95}\text{Zr}$ ,  $^{95}\text{Nb}$  and  $^{103}\text{Ru}$ . The accumulation of these nuclides in tumor tissue was very similar to that of  $^{46}\text{Sc}$ .<sup>14-16</sup> In the case of  $^{51}\text{Cr}$ ,  $^{181}\text{Hf}$  and  $^{182}\text{Ta}$ , very similar results were obtained.<sup>13,15,16</sup> These elements became extremely concentrated in inflammatory tissue.

**Table 1** Classification of metal elements according to accumulated area in tumor tissue<sup>7-9,11-17</sup>

Nuclides	Accumulated areas
$^{22}\text{Na}$	Necrotic tumor tissue
$^{86}\text{Rb}$ , $^{134}\text{Cs}$ , $^{201}\text{Tl}$ $^{65}\text{Zn}$ , $^{103}\text{Pd}$	Viable tumor tissue
$^{67}\text{Ga}$ , $^{111}\text{In}$	Connective tissue (especially inflammatory tissue) > viable tumor tissue > necrotic tumor tissue
$^{169}\text{Yb}$ , $^{167}\text{Tm}$	Viable tumor tissue and tissue containing viable and necrotic tumor tissue > connective tissue > necrotic tumor tissue
$^{46}\text{Sc}$ , $^{51}\text{Cr}$ , $^{103}\text{Ru}$ , $^{95}\text{Zr}$ , $^{181}\text{Hf}$ , $^{95}\text{Nb}$ , $^{182}\text{Ta}$	Connective tissue (especially inflammatory tissue) $\gg$ viable tumor tissue and necrotic tumor tissue

**Table 2** Relationship between metal ions and binding substances (or status) in tumor tissue<sup>7-9,11-17</sup>

Metal ion	Binding substances (or status)
$\text{Na}^+$ , $\text{Rb}^+$ , $\text{Cs}^+$ , $\text{Tl}^+$ (Ions of alkaline metals and Tl)	Exist mostly as a free ion
$\text{Zn}^{2+}$ , $\text{Pd}^{2+}$ (Some borderline and soft acids)	-SH radicals in protein
$\text{Ga}^{3+}$ , $\text{In}^{3+}$ (Trivalent hard acids which are formed by losing electrons from the <i>s</i> -shell and the <i>p</i> -shell)	Acid mucopolysaccharide with a mol. wt. ca. 10,000 daltons
$\text{Yb}^{3+}$ , $\text{Tm}^{3+}$ (Trivalent hard acids which are formed by losing electrons from the <i>f</i> -shell and the <i>p</i> -shell)	Acid mucopolysaccharide with a mol. wt. ca. 10,000 daltons
$\text{Sc}^{3+}$ , $\text{Cr}^{3+}$ , $\text{Zr}^{4+}$ , $\text{Hf}^{4+}$ , $\text{Nb}^{5+}$ , $\text{Ta}^{5+}$ (Tri-, tetra- and pentavalent hard acids which are formed by losing electrons from the <i>d</i> -shell and the <i>s</i> -shell)	Acid mucopolysaccharides with a mol. wt. exceeding 40,000 daltons
$\text{Ru}^{3+}$ (Trivalent borderline acid which is formed by losing electrons from the <i>d</i> -shell and the <i>s</i> -shell)	Acid mucopolysaccharides with a mol. wt. exceeding 40,000 daltons (partly bound)

$^{65}\text{Zn}$  and  $^{103}\text{Pd}$ : Figure 1 shows the result for  $^{65}\text{Zn}$  and  $^{103}\text{Pd}$ . These nuclides accumulated in viable tumor tissue, and were not seen in the necrotic tumor tissue.<sup>17</sup>

#### Classification of metal elements and accumulated area in tumor tissue

Biodistributions of these radioactive nuclides in tumor tissue are summarized in Table 1.  $^{22}\text{Na}$  concentrated in necrotic tumor tissue.  $^{86}\text{Rb}$ ,  $^{134}\text{Cs}$ ,  $^{201}\text{Tl}$ ,  $^{65}\text{Zn}$  and  $^{103}\text{Pd}$  accumulated in viable tumor tissue and were not seen in necrotic tumor tissue.  $^{67}\text{Ga}$  and  $^{111}\text{In}$  were predominant in connective tissue (especially inflammatory tissue) rather than in viable tumor tissue and were hardly seen in necrotic tumor tissue.

$^{169}\text{Yb}$  and  $^{167}\text{Tm}$  accumulated in viable tumor tissue and tissue containing viable and necrotic tumor tissue. The accumulations of these nuclides in tumor tissue differed only slightly from those  $^{67}\text{Ga}$  and  $^{111}\text{In}$ .

The accumulations of  $^{46}\text{Sc}$ ,  $^{51}\text{Cr}$ ,  $^{103}\text{Ru}$ ,  $^{95}\text{Zr}$ ,  $^{181}\text{Hf}$ ,  $^{95}\text{Nb}$  and  $^{182}\text{Ta}$  in connective tissue (especially inflammatory tissue) were much more dominant than those in viable and necrotic tumor tissue.

#### Relation between metal ions and binding substances (or status) in tumor tissue

We reported previously that monovalent cations ( $\text{Na}^+$ ,  $\text{Rb}^+$ ,  $\text{Cs}^+$ ,  $\text{Tl}^+$ ) existed as free ions in the tissue fluids, that  $\text{Ga}^{3+}$ ,  $\text{In}^{3+}$ ,  $\text{Yb}^{3+}$ ,  $\text{Tm}^{3+}$  were bound to the acid mucopolysaccharide with a molecular weight of about ten thousands daltons in the soft tissues, and that  $\text{Cr}^{3+}$ ,  $\text{Sc}^{3+}$ ,  $\text{Ru}^{3+}$ ,  $\text{Zr}^{4+}$ ,  $\text{Hf}^{4+}$ ,  $\text{Nb}^{5+}$  and  $\text{Ta}^{5+}$  were bound to the acid mucopolysaccharides with molecular weights exceeding forty thousand daltons in tissues such as tumor and inflammatory tissues.<sup>8,11-16</sup> It is known that  $\text{Zn}^{2+}$  and  $\text{Pd}^{2+}$  are bound to the SH-radicals in the protein.<sup>18,19</sup> The

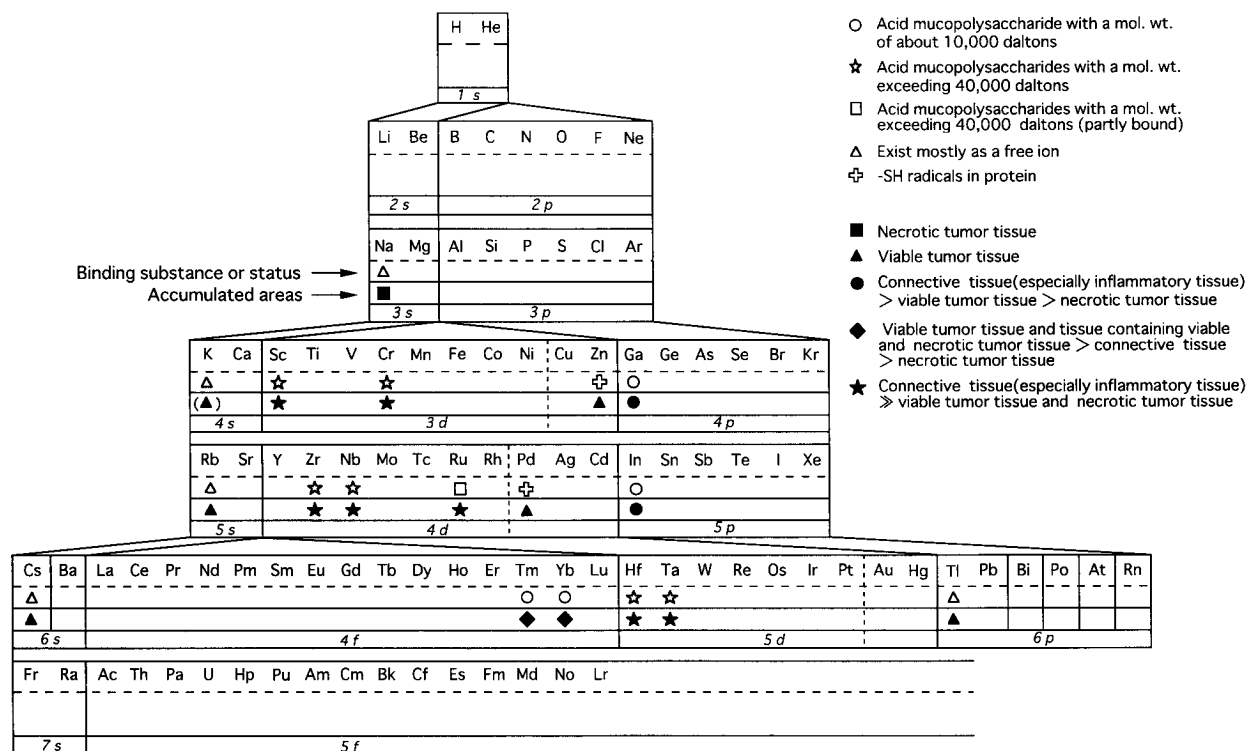


**Fig. 2** Relationship among the location of elements in the Thomsen-Bohr-type periodic table, binding substance (or status), and accumulated area of these elements in tumor tissue. Binding substances and accumulated area for metal ions are shown (below each element in the Thomsen-Bohr-type periodic table).

binding substances (or status) of these metal ions in the tissues are summarized in Table 2.

## DISCUSSION

### Relation between the physicochemical properties of metal ions and their chemical bonds

It is well known that potassium ion (ionic radius 0.133 nm) exists in the intracellular fluid in tissue, sodium ion (0.079 nm) existing in extracellular fluid. We reported previously that monovalent cations ( $Rb^+$ ,  $Cs^+$ ,  $Tl^+$ ) whose ionic radii exceed 0.133 nanometers behave like the potassium ion.<sup>9</sup> Potassium and potassium analogs (rubidium, cesium, thallium) are avidly taken up into viable tumor tissue whose  $Na^+$ ,  $K^+$ -ATPase activity is increased, although sodium is more dominant in necrotic tumor tissue than in viable tumor tissue.

Regarding the chemical bond of metal compounds, the following rules apply.<sup>10</sup> A number of Lewis acids of diverse types are classified as hard acids and soft acids. Hard acids prefer to bind to hard bases. Soft acids prefer to bind to soft bases. Among the ions of the above metals,  $Ga^{3+}$ ,  $In^{3+}$ ,  $Yb^{3+}$ ,  $Tm^{3+}$ ,  $Cr^{3+}$ ,  $Sc^{3+}$ ,  $Zr^{4+}$ ,  $Hf^{4+}$ ,  $Nb^{5+}$  and  $Ta^{5+}$  are hard acids,  $Pd^{2+}$  is a soft acid, and  $Ru^{3+}$ ,  $Zn^{2+}$  are borderline acids.

As is shown in Table 2, Ga and In become trivalent hard

acids by losing electrons from the *s*-shell and the *p*-shell. Yb and Tm become trivalent hard acids by losing electrons from the *f*-shell and the *s*-shell. Ga and In are typical elements. Yb and Tm are contained in the transition elements and called the *f*-block elements. Sc, Cr, Zr, Hf, Nb and Ta become hard acids of tri-, tetra- and penta-valence which are formed by losing electrons from the *d*-shell and the *s*-shell. Ru becomes a borderline acid of trivalence which is formed by losing electrons from the *d*-shell and the *s*-shell. These elements are contained in the transition elements and called the *d*-block elements. Zn becomes a borderline acid of bivalence which is formed by losing electrons from the *s*-shell. Pd becomes a soft bivalent acid which is formed by losing electrons from the *d*-shell.

Among the radicals contained in body constituents,  $R-SO_3^-$ ,  $R-PO_3^{2-}$  and  $R-COO^-$  are hard bases, and  $R-S^-$  and  $R-SH$  are soft bases. It is reasonable to assume that hard acids such as  $Sc^{3+}$ ,  $Cr^{3+}$ ,  $Ga^{3+}$ ,  $In^{3+}$ ,  $Yb^{3+}$ ,  $Tm^{3+}$ ,  $Zr^{4+}$ ,  $Hf^{4+}$ ,  $Nb^{5+}$  and  $Ta^{5+}$  would bind to hard bases such as  $R-SO_3^-$ ,  $R-PO_3^{2-}$  and  $R-COO^-$  in tissue. It is also reasonable to assume that metallothioneins in tissue are composed of  $R-SH$  radicals in protein and soft acids such as  $Pd^{2+}$ . In fact, it is known that metallothioneins in the body are composed of a specific protein and  $Pd^{2+}$ .

It is a well known fact that fibroblasts produce a large

amount of acid mucopolysaccharides (the carbohydrate component of proteoglycan) as the inter-cellular substance in inflammatory tissue, and that these mucopolysaccharides have many carboxy radicals and sulphonic groups in their structure. There is convincing evidence that  $^{67}\text{Ga}^{3+}$  binds to the acid mucopolysaccharide.<sup>11</sup> These ten elements, which become hard acids of tri-, tetra- and penta-valence, behave like  $^{67}\text{Ga}^{3+}$  in tissue.

These results indicate that the difference in intra-tumor distribution of these elements is caused by a difference in the binding substances (or status) of these elements in tissue.

*Relation among the location of elements in the Thomsen-Bohr-type periodic table, binding substances (or status) and area of accumulation of these elements in tumor tissue*

Binding substances (or status) and the area of accumulation of metal ions are shown below each element in the Thomsen-Bohr type periodic table (Fig. 2). For transition elements of the first transition series, the  $3d$ -orbital is filled with electrons from Sc to Ni. In the second transition series, the  $4d$ -orbital is filled with electrons from Y to Rh. In the third transition series, the  $5d$ -orbital is filled with electrons from Lu to Pt. Sc and Cr have incomplete  $3d$ -shells, Zr, Nb and Ru have incomplete  $4d$ -shells, and Hf and Ta have incomplete  $5d$ -shells. These seven elements, which have incomplete  $d$ -shells, were bound to acid mucopolysaccharides whose molecular masses exceed 40,000 daltons. And trivalent hard acids ( $\text{Ga}^{3+}$ ,  $\text{In}^{3+}$ ,  $\text{Yb}^{3+}$  and  $\text{Tm}^{3+}$ ), which have complete  $d$ -shells, were bound to the acid mucopolysaccharide with a molecular mass of about 10,000 daltons.

These results clearly suggest that trivalent hard acids which have complete  $d$ -shells are essentially bound to the acid mucopolysaccharide with a molecular mass of about 10,000 daltons in soft tissues. In addition, most hard acids of tri-, tetra-, and pentavalent and some borderline acids ( $\text{Ru}^{3+}$ , etc.) which have incomplete  $d$ -shells are essentially bound to the acid mucopolysaccharides whose molecular weights exceed 40,000 daltons. It is certain that soft acids (except for some monovalent soft acids) and some borderline acids ( $\text{Zn}^{2+}$ , etc.) are bound to the SH-radicals in protein and exist as components of metallothionein in tissues.<sup>18,19</sup> Most of the  $^{22}\text{Na}$ ,  $^{86}\text{Rb}$  and  $^{134}\text{Cs}$  (alkaline metals), and  $^{201}\text{Tl}$  exists in the free form in tumor tissue. Therefore, the binding substance (or status) of metal ion in the tissue is determined by its physicochemical properties.

In conclusion, the biodistribution of radioactive metal ions in tumor tissue is determined by its own physicochemical properties.

## REFERENCES

1. Kahn H. Ablagerung von aktivem Wismut in malignen Tumoren. *Strahlentherapie* 37: 751-766, 1930.
2. Paterson AHG, McCready VR. Review article: Tumor imaging radiopharmaceuticals. *Br J Radiol* 48: 520-531, 1975.
3. Larson SM. Mechanisms of localization of gallium-67 in tumors. *Semin Nucl Med* 8: 193-203, 1978.
4. Lopez-Majano V, Alvarez-Cerveral J. Neoplasm localization with radionuclides. *Eur J Nucl Med* 4: 313-324, 1979.
5. Ando A, Ando I, Hiraki T, Hisada K. Relation between the location of elements in the periodic table and tumor-uptake rate. *Int J Nucl Med Biol* 12: 115-123, 1985.
6. Ando A, Ando I, Hiraki T, Hisada K. Relation between the location of elements in the periodic table and various organ-uptake rates. *Nucl Med Biol* 16: 57-80, 1989.
7. Ando A, Ando I, Sanada S, Katayama M, Hiraki T, Doishita K, et al. Study of the distribution of tumor affinity metal compounds and alkaline metal compounds in the tumor tissues by macroautoradiography. *Int J Nucl Med Biol* 11: 195-201, 1984.
8. Ando A, Ando I, Sakamoto K, Hiraki T, Hisada K, Takeshita M. Affinity of  $^{167}\text{Tm}$ -citrate for tumor and liver tissue. *Eur J Nucl Med* 8: 440-446, 1983.
9. Ando A, Ando I, Katayama M, Sanada S, Hiraki T, Mori H, et al. Biodistributions of radioactive alkaline metals in tumor bearing animals: comparison with  $^{201}\text{Tl}$ . *Eur J Nucl Med* 14: 352-357, 1988.
10. Pearson RG. Physical and inorganic chemistry. *J Am Chem Soc* 85: 3533-3539, 1963.
11. Ando A, Ando I, Hiraki T, Takeshita M, Hisada K. Mechanism of tumor and liver concentration of  $^{67}\text{Ga}$ :  $^{67}\text{Ga}$  binding substances in tumor tissues and liver. *Int J Nucl Med Biol* 10: 1-9, 1983.
12. Ando A, Ando I, Hiraki T, Takeshita M, Hisada K. Mechanism of tumor and liver concentration of  $^{111}\text{In}$  and  $^{169}\text{Yb}$ :  $^{111}\text{In}$  and  $^{169}\text{Yb}$  binding substances in tumor tissues and liver. *Eur J Nucl Med* 7: 298-303, 1982.
13. Ando A, Ando I, Yamada N, Hiraki T, Hisada K. Distribution of  $^{46}\text{Sc}$  and  $^{51}\text{Cr}$  in tumor-bearing animals and the mechanism for accumulation in tumor and liver. *Nucl Med Biol* 14: 143-151, 1987.
14. Ando A, Ando I, Hiraki T, Hisada K. Distribution of  $^{103}\text{Ru}$ -chloride in tumor-bearing animals and the mechanism for accumulation in tumor and liver. *Nucl Med Biol* 15: 133-140, 1988.
15. Ando A, Ando I. Distribution of  $^{95}\text{Zr}$  and  $^{181}\text{Hf}$  in tumor-bearing animals and mechanism for accumulation in tumor and liver. *Nucl Med Biol* 13: 21-29, 1986.
16. Ando A, Ando I. Biodistribution of  $^{95}\text{Nb}$  and  $^{182}\text{Ta}$  in tumor-bearing animals and mechanisms for accumulation in tumor and liver. *J Radiat Res* 31: 97-109, 1990.
17. Ando A, Ando I. Biodistribution of radioactive bipoisitive metal ions in tumor-bearing animals. *BioMetals* 7: 185-192, 1994.
18. Piscator M, Lind B. Cadmium, zinc, copper, and lead in human renal cortex. *Arch Environ Health* 24: 426-431, 1972.
19. Winge DR, Premakumar R, Rajagopalan KV. Metal-induced formation of metallothionein in rat liver. *Arch Biochem Biophys* 170: 242-252, 1975.

1. Kahn H. Ablagerung von aktivem Wismut in malignen